Thermochimica Acta 474 (2008) 41–46

Contents lists available at ScienceDirect

Thermochimica Acta

journal homepage: www.elsevier.com/locate/tca

Mechanism and kinetics of crystallization of α-Fe in amorphous $Fe_{81}B_{13}Si_4C_2$ alloy

D.M. Minić*, B. Adnađević

Faculty of Physical Chemistry, University of Belgrade, Strudentski trg 12-16, 11001 Belgrade, Serbia

ARTICLE INFO

Article history:
Received 13 March 2008
Received in revised form 14 May 2008
Accepted 25 May 2008
Available online 7 July 2008

Keywords:
Amorphous alloy
Activation energy

ABSTRACT

The non-isothermal crystallization of α-Fe from $Fe_{81}B_{13}Si_4C_2$ amorphous alloy was investigated. The kinetic parameters of crystallization process were determined by Kissinger and Kissinger–Akahira–Sunose (KAS) methods. It was established that the kinetic parameters of transformation do not change with the degree of crystallization in the range of 0.1–0.7. The kinetic model of the crystallization process was determined using the Malek's procedure. It was established that the primary crystallization α-Fe phase from amorphous alloy can be described by Šesták–Berggren autocatalytic model with kinetic triplet $E_a = 349.4.0\ kJ\ mol^{-1}$, $\ln A = 50.76$ and $f(\alpha) = \alpha^{0.72}(1-\alpha)^{1.02}$.

1. Introduction

Amorphous alloys are relatively new materials offering a specific combination of properties and attracting special interest of many scientists during the last two decades. The metallic glasses of Fe and Co alloys have attracted much attention since exhibiting soft ferromagnetic properties which made them very applicable in different devices, including transformers, sensors, magnetic tapes and heads of recorder [1–5].

The amorphous state of matter is, however, structurally and thermodynamically unstable and very susceptible to partial or complete crystallization during thermal treatment or non-isothermal compacting which is followed by change in their structural and physical properties [6]. The crucial limitation with respect to using amorphous alloys for high temperature applications arises from their restricted thermal stability. The onset of exothermic crystallization upon crossing the stability domain of the glassy state results in the formation of highly stable, but brittle intermetallic compounds, which renders these alloys useful only once. The latter imposes the knowledge of the alloys stability in a broad range of temperatures due to different crystallization processes, which appears during heating.

There are three important modes of crystallization involving nucleation and growth processes, depending on the composition of a particular alloy: the polymorphous crystallization, primary crystallization and eutectic crystallization [7]. The *polymorphous crystallization* occurs without any change of composition so there is no concentration difference across the reaction front. *Primary crystallization* is the process in which a phase of one of the alloy constituents first crystallizes. The dispersed primary crystallized phase coexists with the amorphous matrix and may serve as the nucleation site for secondary or tertiary crystallization. *Eutectic crystallization* is the simultaneous crystallization of two crystalline phases by discontinuous reactions.

The crystallization of a metallic glass upon heating is induced in several ways. In calorimetric measurements, two basic methods are in use, isothermal and non-isothermal. However, the results of the crystallization process can be explained in terms of several theoretical models [8].

The present paper gives a detailed study of the crystallization kinetic of the $Fe_{81}B_{13}Si_4C_2$ amorphous alloy in forms of ribbon. The kinetic parameters of the glass-crystallization transformation were investigated under non-isothermal conditions applying two different methods: classic and isoconversion.

2. Experimental procedure

2.1. Materials and methods

The ribbon shaped samples of $Fe_{81}B_{13}Si_4C_2$ amorphous alloy were obtained using the standard procedure of rapid quenching of the melt on a rotating disc (melt-spinning). The obtained ribbon was 2 cm wide and 35 μm thick.

The crystallization process was investigated by the differential scanning calorimetry (DSC) in a nitrogen atmosphere using SHIMADZU DSC-50 analyzer. In this case, samples weighing several

* Corresponding author. Tel.: +381 11 3336 689; fax: +381 11 187 133.
E-mail address: dminic@ffh.bg.ac.yu (D.M. Minić).

0040-6031/$ – see front matter © 2008 Elsevier B.V. All rights reserved.
doi:10.1016/j.tca.2008.05.010

milligrams were heated in the DSC cell from room temperature to 650 °C in a stream of nitrogen with a flowing rate of 20 mL min^{-1} and at the heating rates of 5, 10, 20 and 30 K min^{-1}.

In order to investigate the structural transformations by X-ray diffraction (XRD), the samples of amorphous alloy $Fe_{81}B_{13}Si_4C_2$ were annealed at the different temperatures, in the temperature range of 473–1103 K, in a stream of nitrogen during 30 min. The X-ray powder diffraction patterns for as-prepared alloy as well as for annealed samples were recorded on a Philips PW-1710 automated diffractometer using a Cu tube operated at 40 kV and 30 mA. The instrument was equipped with a diffracted beam curved graphite monochromator and Xe-filled proportional counter. For the routine characterization, the diffraction data was collected in the range of 2θ Bragg angles (4–100° counting for 0.1 s). Silicon powder was used as an external standard for calibration of diffractometer. All XRD measurements were done with solid samples in a form of ribbon at ambient temperature.

3. Kinetic analysis

The kinetic information can be obtained from dynamic experiments by means of various methods. The methods of thermal analysis, such as DTA or DSC, are very popular for kinetic analysis of crystallization processes in amorphous solids. All kinetic studies assume that the isothermal rate of conversion $d\alpha/dt$, is a linear function of the temperature-dependent rate constant, $k(T)$, and a temperature-independent function of the conversion, $f(\alpha)$, that is

$$\frac{d\alpha}{dt} = k(T)f(\alpha), \tag{1}$$

where t represents time, α is the extent of reaction, T is the temperature, $k(T)$ is the temperature-dependent rate constant and $f(\alpha)$ is a function that represents the reaction model [9].

According to Arrhenius's equation, the temperature-dependent rate constant, $k(T)$ is defined as

$$k(T) = A\exp\left(-\frac{E_a}{RT}\right), \tag{2}$$

where A is the pre-exponential factor independent of temperature, E_a is the activation energy and R is the gas constant.

From these equations, the relation obtained was

$$\frac{d\alpha}{dt} = A\exp\left(-\frac{E_a}{RT}\right)f(\alpha). \tag{3}$$

The extent of reaction (α) is deduced from DSC measurements using Borchardt's assumption [10]:

$$\alpha = \frac{\Delta H(t)}{\Delta H} \Leftrightarrow \frac{d\alpha}{dt} = \frac{1}{\Delta H}\frac{dH}{dt}, \tag{4}$$

where $\Delta H(t)$ and ΔH are the partial and total integrals of the measured signal, respectively; dH/dt is the rate of the transformation heat power.

By drawing the straight line between the beginning and the end of the peak as the baseline, it is always possible to obtain α and $d\alpha/dt$ from DSC curves. Eq. (4) shows that the rate of conversion $d\alpha/dt$ is proportional to the measured specific heat flow. For non-isothermal measurements at constant heating rate $\beta = dT/dt$, Eq. (3) is transformed to

$$\beta\frac{d\alpha}{dT} = A\exp\left(-\frac{E_a}{RT}\right)f(\alpha), \tag{5}$$

where $d\alpha/dt \equiv \beta(d\alpha/dT)$.

The overall activation energy of crystallization of an amorphous alloy under linear heating condition can be determined by the Kissinger as well as by the Ozawa peak methods relating on the dependence of the exothermic peak temperature T_p on the heating rate β [11].

Kissinger [12] proposed that the activation energy can be determined according to the equation:

$$\ln\left(\frac{\beta}{T_p^2}\right) = \ln\left(\frac{AR}{E_a}\right) - \frac{E_a}{RT_p}. \tag{6}$$

In this case, the plot of $\ln(\beta/T_p^2)$ versus $1/T_p$ yields a straight line with a slope of $-E_a/R$ and an intercept of $\ln(AR/E_a)$.

For the determination of the activation energy in non-isothermal conditions Ozawa [13] proposed the equation:

$$\ln\beta = \ln\frac{AE_a}{R} - 1.0516\frac{E_a}{RT_p}, \tag{7}$$

where the plot of $\ln(\beta)$ versus $1/T_p$ yields a straight line with a slope of $-E_a/R$ and an intercept of $\ln(AE_a/R)$.

On the basis of dynamic DSC measurements for different heating rates, isoconversional method of Kissinger–Akahira–Sunose (KAS) method enabling the determination values of E_a over a wide range of conversions α without knowing the conversion function was also used [12,14]. This model known as "model-free method", involves measuring the temperatures T_α corresponding to fixed values of the crystallized volume fraction, α, for different heating rates, β, and the plotting $\ln\beta$ against $1/T^\alpha$, according to the equation:

$$\ln\left(\frac{\beta}{T_\alpha^2}\right) = \ln\left(\frac{AR}{E_{a(\alpha)}}F(\alpha)\right) - \frac{E_{a(\alpha)}}{RT_\alpha}. \tag{8}$$

The left-hand side of Eq. (8) is linear with respect to the inverse temperature, $1/T_\alpha$, and enables the activation energy to be evaluated by using a linear regression method. In the case of a single step process, a constant value of $E_{a(\alpha)}$ is obtained, while the dependence of $E_{a(\alpha)}$ upon α indicates a complex process involving more than one step having different activation energies [15].

General equation enabling the analysis of conversion kinetics involving nucleation and growth in solid phase was proposed by Avrami [16]:

$$\alpha(t) = 1 - \exp[-(kt)^n], \tag{9}$$

where $k = k_0\exp(-E_a/RT)$, $\alpha(t)$ is a degree of transformed volume, n is a kinetic exponent.

Differentiation of this equation with respect to time gives the rate equation usually known as the JMA equation:

$$\frac{d\alpha}{dt} = kn(1-\alpha)[-\ln(1-\alpha)]^{1-1/n}. \tag{10}$$

The JMA equation is based on assumptions of isothermal crystallization, homogenous nucleation or heterogeneous nucleation at randomly dispersed particles of the second phase. The growth rate of the new phase is independent of time and controlled by temperature and low anisotropy of growing crystals. However if the entire nucleation process takes place during the early stage of transformation and becomes negligible afterward, the JMA equation can also be applied in non-isothermal conditions [17].

The validity of listed assumptions is not given a priori, and a simple and reliable testing method was developed [18,19]. Once the apparent activation energy has been determined, it is possible to find the kinetic model which best describes the measured set of thermoanalytical data. It can be shown that, for this purpose, it is useful to define two special functions $y(\alpha)$ and $z(\alpha)$, which can easily be obtained by a simple transformation of the experimental data. The conversions, in which the $y(\alpha)$ and $z(\alpha)$ functions exhibit the maximum values are designated as α_y^* and α_z^*, respectively. In non-isothermal conditions, these functions can be expressed as follows

[18–20]:

$$y(\alpha) = \left(\frac{d\alpha}{dt}\right) \exp\left(\frac{E_a}{RT}\right) = Af(\alpha), \quad (11)$$

$$z(\alpha) \approx \left(\frac{d\alpha}{dt}\right) T^2. \quad (12)$$

The maximum of the $y(\alpha)$ function for the JMA model depends on the value of the kinetic exponent:

$$\alpha_y^* = 0 \quad \text{for } n \leq 1,$$

$$\alpha_y^* = 1 - \exp(n^{-1} - 1) \quad \text{for } n > 1.$$

The value of α_y^* is always lower than the maximum of value for α_z^*. For JMA model, $\alpha_z^* = 0.632$. This value is a characteristic "fingerprint" of the JMA model, and it can be used as a simple test of the applicability of this model.

If the $y(\alpha)$ function exhibits a maximum in interval $\alpha_y^* \in (0, \alpha_z)$ and $\alpha_z^* \neq 0.632$, the empirical Šesták–Berggren kinetic model gives the best description of the investigated process [21,22]. This model is based on the equation:

$$f(\alpha) = \alpha^M (1-\alpha)^N, \quad (13)$$

where M and N represents the kinetic exponents.

In this case, the expression for reaction rate of the investigated crystallization process can be given as

$$\frac{d\alpha}{dt} = A \exp\left(-\frac{E_a}{RT}\right) \alpha^M (1-\alpha)^N. \quad (14)$$

For this model, the ratio of the kinetic parameter $p = M/N$ can be calculated from the maximum of the $y(\alpha)$ function [20]:

$$p = \frac{M}{N} = \frac{\alpha_y^*}{1-\alpha_y^*} \quad (15)$$

Introducing this equation in Eq. (14) gives

$$\ln\left[\left(\frac{d\alpha}{dt}\right) \exp\left(\frac{E_a}{RT}\right)\right] = \ln A + N \ln[\alpha^p (1-\alpha)]. \quad (16)$$

This equation very well describes the processes of nucleation and growth in non-crystalline solids. The parameters M and N define relative contributions of acceleratory and decay regions of the kinetic process. From the linear dependence $\ln[(d\alpha/dt)\exp(E_a/RT)] = f(\ln[\alpha^p(1-\alpha)])$, it could be possible to obtain the kinetic exponent N and the pre-exponential factor, $\ln A$. The value of kinetic exponent M then can be obtained directly from Eq. (15).

4. Results and discussion

The crystallization kinetics of α-Fe in the amorphous alloy was studied by differential scanning calorimetry at different heating rates of the alloy (5, 10, 20 and 30 K min^{-1}).

Fig. 1 shows the continuous DSC curves of $Fe_{81}B_{13}Si_4C_2$ ribbon taken at four different heating rates.

All the DSC curves have a single well-formed exothermic peak representing crystallization in the temperature range 770–830 K. The exothermal peaks are significantly shifted to higher temperatures with an increasing heating rate. This is in accordance with the presumption about the thermal activation of the crystallization process. The influence of the heating rate on the values of initial, T_i, maximal, T_p and final T_f temperatures is shown in Table 1. The shape of DSC curves depends on the heating rate, too. The values of shape factor, S, obtained as the ratio of half-widths of crystallization peak for a particular heating rate, are presented in the same table together with the values of kinetic parameters, the overall

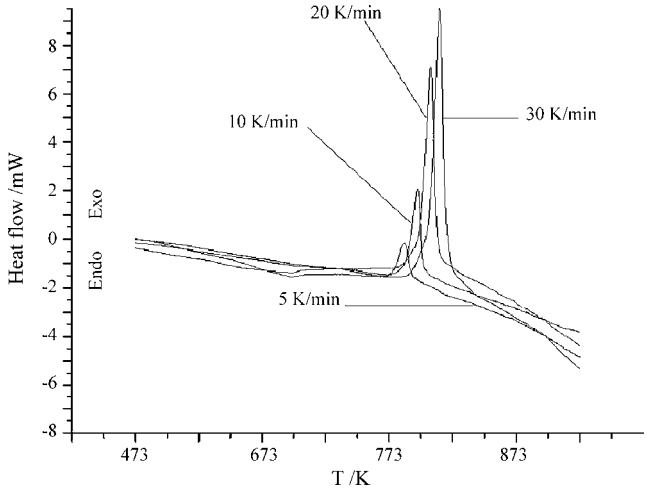

Fig. 1. DSC curves for $Fe_{81}B_{13}Si_4C_2$ ribbon at different heating rates.

apparent activation energy and pre-exponential factor calculated by Kissinger's and Ozawa's methods.

According to the values of shape factor S, asymmetry of conversions curves increases with the decrease of heating rates indicating that the heating rate have a strong influence on crystallization process which can occur in more than one step.

Fig. 2 shows the XRD patterns of the $Fe_{81}B_{13}Si_4C_2$ amorphous ribbon as prepared and after isothermal annealing the different isothermal temperatures (298, 473, 673, 823, 873 and 1103 K).

The presence of only a spread halo at the 2θ range of 20–45° suggests an amorphous structure of as-prepared alloy. The diffraction pattern of alloy annealed at the temperature of $T = 473$ K shows beside of a spread halo and one very sharp peak at $2\theta = 83.4$ °C indicating the presence of a crystal phase in a matrix of an amorphous phase. The increase of the annealed temperature results in an increase of the peak intensity. Starting from temperature $T = 823$ K, the diffractograms show a new sharp peak with the

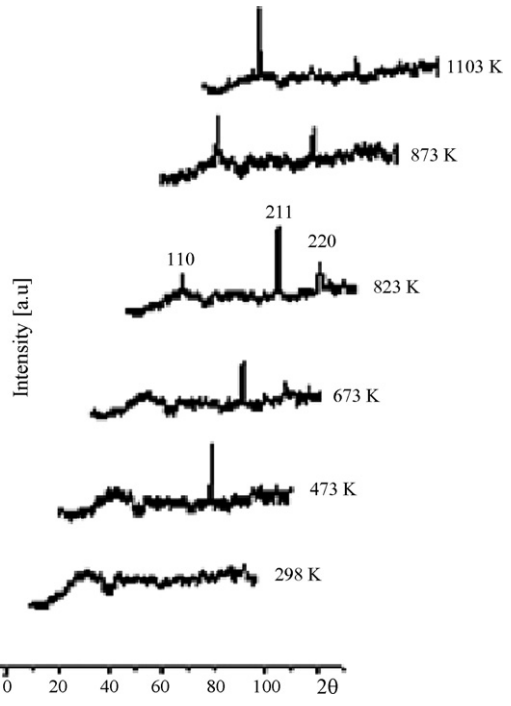

Fig. 2. XRD patterns for the alloy annealed at different temperatures.

Table 1
The values of T_i, T_p, T_f and S for the amorphous $Fe_{81}B_{13}Si_4C_2$ alloy upon continuous heating at different heating rates

β (K min^{-1})	T_i (K)	T_p (K)	T_f (K)	S	Ozawa		Kissinger	
					E_a (kJ mol^{-1})	A ($\times 10^{22}$ min^{-1})	E_a (kJ mol^{-1})	A ($\times 10^{21}$ min^{-1})
5	765	785	815	0.59				
10	774	793	819	0.59				
20	782	804	827	0.70	338.0 ± 1.8	1.10 ± 2.28	351.2 ± 1.8	3.06 ± 2.28
30	786	811	833	0.75				

maximum located at $2\theta = 45.3^\circ$. A further increase of the annealing temperature causes an increased intensity of that peak and a decrease of its half width indicating the increase of crystallinity of alloy. Thoroughly studying diffractograms by the comparative semi-qualitative analysis of annealed alloy, according to JPCDS card no. 06 6698, gives evidence of the presence of α-Fe crystals in annealed alloy beside an amorphous phase indicating the primary crystallization amorphous alloy during heating.

These results show that probably even at ambient temperature, in the alloy exists highly disordered α-Fe clusters which being ordered by annealing already at 673 K. The annealing of alloy at the temperatures in the range of 673–823 K, leads further to the ordering of structure. The dimensions and concentrations of the formed α-Fe nuclei at $T = 823$ K are enough to cause a spontaneous growing of α-Fe nuclei. The rate of nuclei growth increases with the increasing of annealing temperature of the considered alloy.

In order to establish the influence of fractional extent of reaction α on the values of kinetic parameters we applied the isoconversion method, according to the Kissinger–Akahira–Sunose [12,14]. According to this method, a linear relationship of $\ln(\beta/T^2)$ versus $1/T$ was established, describing well data from non-isothermal DSC measurements at the α range of 0.1–0.7. The values of the apparent activation energy and the intercepts $\ln[ARf(\alpha)/E_a]$ calculated by means of this method are pointed out in Fig. 3.

It can be observed that the determined apparent activation energy as well intercepts $\ln[ARf(\alpha)/E_a]$ for the crystallization process of α-Fe in the amorphous $Fe_{81}B_{13}Si_4C_2$ alloy are practically constant at the α range of 0.1–0.7. This suggests that the apparent activation energy as well as the pre-exponential factor depends on the same way on the crystallization degree of considered process. That could be an indication of a single step reaction. The average value of the apparent activation energy was found to be $E_a = 352.4 \pm 1.8$ kJ mol^{-1}.

The crystallization kinetics of the amorphous solids involving the nucleation and growth of nuclei is usually interpreted by the JMA model. The validity of this model was investigated using the normalized $y(\alpha)$ and $z(\alpha)$ functions proposed by Malek [18–20], Fig. 4.

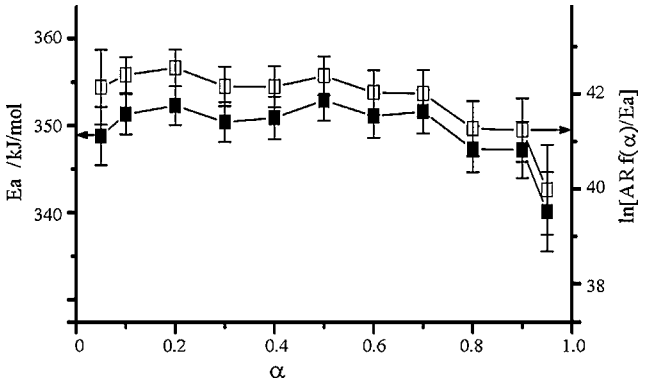

Fig. 3. The apparent activation energies (E_a) and the intercepts as function of the crystallized fraction α.

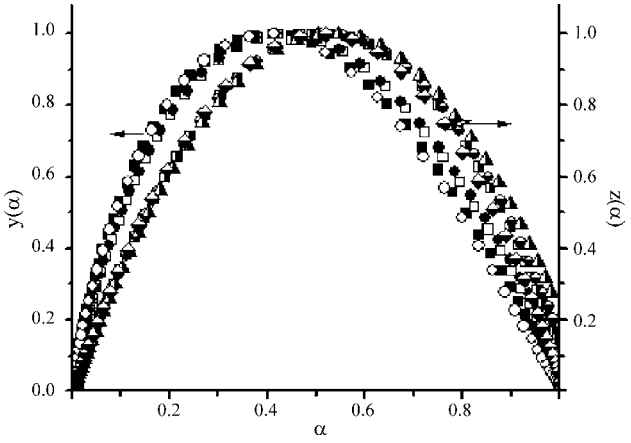

Fig. 4. Normalized $y(\alpha)$ and $z(\alpha)$ functions at the different heating rates.

The obtained normalized functions $y(\alpha)$ and $z(\alpha)$ are independent on the heating rate, β, and the both functions exhibit the well-defined maxima which were located at an exactly defined value of α (α_y^* for the $y(\alpha)$ function and α_z^* for $z(\alpha)$ function, respectively), Table 2.

From Table 2, it can be seen that the values of α_y^* fall into the range $\alpha_y^* \in (0, \alpha_z)$ ($0.41 \leq \alpha_y^* \leq 0.42$) and the values of α_z^* are less than 0.632 ($0.51 \leq \alpha_z^* \leq 0.55$). From the obtained results, it follows that the conditions of validity of the JMA model are not fulfilled for the crystallization of α-Fe in an amorphous $Fe_{81}B_{13}Si_4C_2$ alloy. The displacement α_z^* in the range lower values indicates the complexity of the process and can be caused by the influence of surface nucleation or by the affect of released crystallization heat on the temperature distribution within a sample. However, the relatively high value of α_y^* indicates an increasing effect of the crystallized phase to overall crystallization kinetics where the crystallized phase further promotes the rate of the crystallization. Such autocatalytic behavior can be well described by means of an empirical two parameter Šesták–Berggren's kinetic model, according to Eq. (13).

Table 3 lists the values of kinetic exponents M and N, as well as the values of $\ln A$ obtained by the procedure described above, for the considered crystallization process at different heating rates.

The obtained values of kinetic exponents M and N are slightly changed with the heating rate β. The values of M vary in the range of $0.64 \leq M \leq 0.81$ with the average value of $M_{av} = 0.72$. The values of N vary in the range of $0.89 \leq N \leq 1.17$ with the average value of $N_{av} = 1.02$. The values of the pre-exponential factor ($\ln A$) in the lim-

Table 2
The maximum of α_y and α_z for the different heating rates

β (K min^{-1})	α_y^*	α_z^*
5	0.41 ± 0.01	0.53 ± 0.01
10	0.42 ± 0.01	0.51 ± 0.01
20	0.42 ± 0.01	0.55 ± 0.03
30	0.41 ± 0.01	0.52 ± 0.01

Table 3
The kinetic exponents *M* and *N* at different heating rates

β (°C min^{-1})	*M*	*N*	ln*A* (min^{-1})
5	0.75 ± 0.03	1.08 ± 0.10	52.85 ± 0.06
10	0.66 ± 0.05	0.92 ± 0.05	53.03 ± 0.10
20	0.64 ± 0.05	0.89 ± 0.07	52.90 ± 0.07
30	0.81 ± 0.10	1.17 ± 0.04	53.02 ± 0.10
Average	0.72 ± 0.06	1.02 ± 0.07	52.95 ± 0.08

its of the experimental error are independent on the heating rate (β). It was shown that this two parameter autocatalytic model is physically meaningful only for $M < 1$ [22]. The JMA model is only a specific case of one general model where the entire nucleation process takes place during the early stages of the transformations, becoming negligible afterward. In that case, the crystallization rate is defined only by temperature and does not depend on the previous thermal history of alloy.

In order to check the established kinetic model, we applied the "Master-plot" method [23,24] (Fig. 5). Using as a reference point value at $\alpha = 0.5$, the following differential master equation is easily derived from Eq. (3):

$$\frac{f(\alpha)}{f(0.5)} = \frac{\mathrm{d}\alpha/\mathrm{d}t}{(\mathrm{d}\alpha/\mathrm{d}t)_{0.5}} \frac{\exp\ (E_a/RT)}{\exp(E_a/RT_{0.5})}, \quad (17)$$

where $(\mathrm{d}\alpha/\mathrm{d}t)_{0.5}$, $T_{0.5}$ and $f(0.5)$ are the reaction rate, the temperature reaction and the differential conversion function, respectively at $\alpha = 0.5$.

The left side of Eq. (17), is a reduced theoretical curve which is characteristic of each kinetic function. The right side of the equation is associated with the reduced rate and can be obtained from experimental data if the apparent activation energy is known and remains constant throughout the reaction. Comparison of both sides of Eq. (17) tells us which kinetic model describes an experimental reaction process.

It can be seen that by using the average value for the apparent activation energy determined from Kissinger–Akahira–Sunose isoconversional method, the suggested kinetic model works very well in the entire conversion range. Therefore, the Šesták–Berggren autocatalytic model represents the best reaction model for describing the crystallization process of α-Fe in the amorphous $Fe_{81}B_{13}Si_4C_2$ alloy.

The crystallization kinetics of amorphous solids is usually interpreted in terms of the Johnson–Mehl–Avrami (JMA) model. However, strictly speaking, this model is valid in isothermal conditions, and it can be rigorously applied to the transformations involving a nucleation and a growth only in a limited number of special cases in non-isothermal conditions. An example of a system which allows the non-isothermal application of the JMA models is one in which the entire nucleation process takes place during the early stages of the transformation, and it becomes negligible afterward. In this case, the crystallization rate is defined only by the temperature and does not depend on the previous thermal history of alloy.

The higher value of *N* exponent designates that the decisive influence on the kinetics of transformation has the formed crystallization phase and the rate of growth. In the propagation process, on account of overlapping of nuclei in growing, it comes to retard of crystallization rate. Bearing in mind the above facts, we can assume that in the amorphous alloy, the α-Fe embryos already exist and at $T \leq 823$ K and at $T \geq 823$ K, these embryos are momentarily transformed into nuclei. The established acceleration of the crystallization process is a consequence of the significant increase of strains in the alloy, which arise on account of α-Fe formation process.

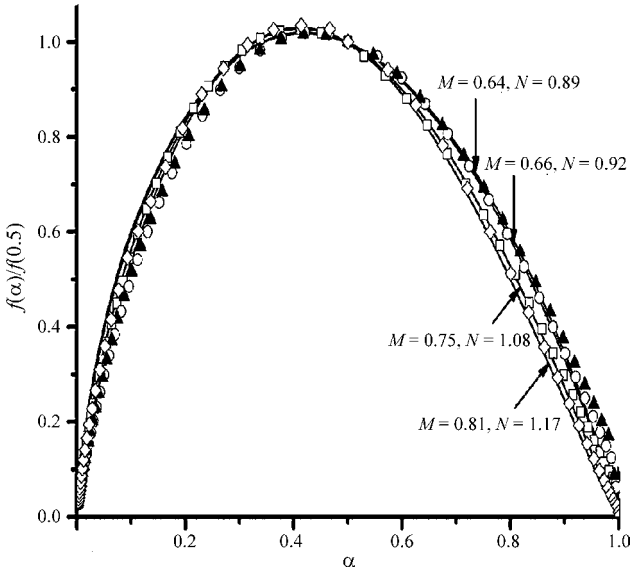

Fig. 5. The theoretical (solid line) and experimental differential master plots of $f(\alpha)/f(0.5)$ versus α for different heating rates: (□) 5 K min^{-1}; (○) 10 K min^{-1}; (▲) 20 K min^{-1}; (◊) 30 K min^{-1}.

5. Conclusions

Kinetics of crystallization of α-Fe from amorphous $Fe_{81}B_{13}Si_4C_2$ alloy can be described by the Šesták–Berggren's kinetic model with the following expression for the reaction rate: $\mathrm{d}\alpha/\mathrm{d}t = 1.11 \times 10^{22} \exp(-349.4/RT)\alpha^{0.72}(1-\alpha)^{1.02}$. At $T \geq 823$ K it comes to instantaneous nucleation of embryos which already exist in the crystallization nuclei of α-Fe. The acceleration of the crystallization process is a consequence of strains in the material which arise on account of the formation of α-Fe. On the other hand, the decrease of the transformation rate is a consequence of an overlapping of the growing α-Fe nuclei.

Acknowledgement

The investigation was partially supported by the Ministry of Science and Environmental Protection of Serbia, under the following Project 142025.

References

[1] N. Cowlam, J. Non-Cryst. Solids 205–207 (1996) 567.
[2] K. Biswas, S. Ram, L. Schultz, J. Eckert, J. Alloy Compd. 397 (2005) 104.
[3] D.S. Santos, R.S. de Biasi, J. Alloy Compd. 335 (2002) 266.
[4] T. Gloriant, S. Surinach, M.D. Baro, J. Non-Cryst. Solids 333 (2004) 320.
[5] J. Bednarčik, R. Nicula, M. Stir, E. Burkel, J. Magn. Magn. Mater. 316 (2007) e823.
[6] D.M. Minić, A. Maričić, R.Z. Dimitrijević, M.M. Ristić, J. Alloy Compd. 430 (2007) 242.
[7] A. Hsiao, M.E. McHenry, D.E. Laughlin, M.J. Kramer, C. Ashe, T. Ohkubo, IEEE Trans. Magn. 38 (5) (2002) 3039.
[8] S. Vyazovkin, C.A. Wight, Int. Rev. Phys. Chem. 17 (1998) 407.
[9] M.E. Brown, D. Dolimore, A.K. Galwey, Reactions in the Solid State. Comprehensive Chemical Kinetics, vol. 22, Elsevier, Amsterdam, 1980.
[10] H.J. Borchardt, F. Daniels, J. Am. Chem. Soc. 78 (1957) 41.
[11] Z.-Z. Yuan, X.-D. Chen, B.-X. Wang, Y.-J. Wang, J. Alloy Compd. 407 (2006) 163.
[12] H.E. Kissinger, Anal. Chem. 29 (1957) 1702.
[13] T. Ozawa, J. Therm. Anal. 2 (1970) 301.
[14] T. Akahira, T. Sunose, Res. Rep. Chiba Inst. Technol. 16 (1971) 22.
[15] A.A. Soliman, S. Al-Heniti, A. Al-Hajry, M. Al-Assiri, G. Al-Barakati, Thermochim. Acta 413 (2004) 57.
[16] M. Avrami, J. Chem. Phys. 7 (1939) 1103.
[17] D.W. Henderson, J. Therm. Anal. 15 (1979) 325.

[18] J. Málek, Thermochim. Acta 267 (1995) 61.
[19] J. Málek, Thermochim. Acta 200 (1992) 257.
[20] J. Málek, Thermochim. Acta 355 (2000) 239.
[21] J. Šesták, G. Berggren, Thermochim. Acta 3 (1971) 1.
[22] J. Málek, J.M. Criado, J. Šesták, J. Militky, Thermochim. Acta 153 (1989) 429.
[23] J.M. Criado, L.A. Pérez-Maqueda, F.J. Gotor, J. Málek, N. Koga, J. Therm. Anal. Calor. 72 (2003) 901.
[24] F.J. Gotor, J.M. Criado, J. Málek, N. Koga, J. Phys. Chem. A 104 (2000) 10777.